

Numerical Study of Cosmic Censorship in String Theory

M. Gutperle

Department of Physics and Astronomy, UCLA, Los Angeles, CA 90095, USA

E-mail: gutperle@physics.ucla.edu

P. Kraus

Department of Physics and Astronomy, UCLA, Los Angeles, CA 90095, USA

E-mail: pkraus@physics.ucla.edu

ABSTRACT: Recently Hertog, Horowitz, and Maeda have argued that cosmic censorship can be generically violated in string theory in anti-de Sitter spacetime by considering a collapsing bubble of a scalar field whose mass saturates the Breitenlohner-Freedman bound. We study this system numerically and find that for various choices of initial data black holes form rather than naked singularities, implying that in these cases cosmic censorship is upheld.

Contents

1. Introduction	1
2. Equations of motion	2
3. Results	5
3.1 Standard boundary conditions	6
3.2 Dirichlet boundary conditions	10
4. Discussion	13

1. Introduction

Inasmuch as they mark a breakdown of classical general relativity, spacetime singularities pose an important challenge to theories of quantum gravity such as string theory. Singularities are common occurrences in the study of cosmology and black holes, but their correct physical description still seems to be beyond our grasp. Penrose proposed the concept of cosmic censorship, which states that singularities which are formed by nonsingular initial data are always hidden behind a horizon [1].

In the case of cosmology it has proven quite challenging to find controlled examples within string theory [2][3][4][5][6][7][8] [9], while for black holes the existence of the event horizon makes it difficult to study the physics of the singularity itself [10][11][12][13][14].

To make progress it would be very helpful to find a naked singularity within a well understood background of string theory. Finding a naked singularity in an anti-de Sitter background would be especially promising, as the nonperturbative tools of the AdS/CFT correspondence could be brought to bear on the problem. An interesting proposal for obtaining such singularities was put forward in a recent paper by Hertog, Horowitz and Maeda (HHM) [15] (see also [16]). Their argument uses the special properties of scalar fields which saturate the Breitenlohner-Freedman bound [17][18], which describes how tachyonic a field in AdS can be without leading to an instability. If one starts with a large and homogeneous bubble of such a scalar field the resulting evolution leads to a singularity in finite time. To argue that the singularity is naked, HHM claim that the energetics of the system is such that no black holes can form.

In this paper we present results on the numerical study of such collapsing bubbles. For all the cases we have studied, we will see that the evolution is consistent with the formation of black holes rather than naked singularities. HHM have actually considered two distinct scenarios. For the first, one imposes standard boundary conditions in AdS, and the argument revolves around the fact that the initial data has negative mass; black holes

on the other hand have positive mass, which might seem to prevent them from forming from the assumed initial data. However, there is a loophole: this definition of the mass is not conserved, as HHM themselves point out. Numerically we will find that the mass rapidly becomes positive, and that a trapped surface subsequently forms outside the bubble. In the second scenario HHM impose Dirichlet boundary conditions at some cutoff position inside AdS. In this case, the mass is conserved, but one also has to consider the possible existence of hairy black holes whose mass is lower than that of the initial data (the no hair theorem does not apply in the presence of the cutoff). We will compare the mass of the black hole with the mass of the initial data for various choices of parameters and find that black holes have sufficiently small mass to form. Similarly, our numerical investigations of the collapsing bubble with Dirichlet boundary conditions again leads to the conclusion that black holes form rather than naked singularities. Thus, for all the examples we have studied cosmic censorship is upheld. However, we should note that we have by no means exhausted all possible choices of parameters, including some suggested in [15], and so it is possible that cosmic censorship can be violated in some other regime.

2. Equations of motion

We consider the action for a scalar field coupled to gravity in 5 dimensions with a negative cosmological constant,

$$S = \int d^5x \sqrt{-g} \left(\frac{1}{2} R + 6 - \frac{1}{2} (\partial\phi)^2 - V(\phi) \right). \quad (2.1)$$

The potential corresponding to a free scalar which saturates the Breitenlohner-Freedman bound is

$$V(\phi) = -2\phi^2. \quad (2.2)$$

For now we will assume 2.2, although we will also consider the full potential arising in supergravity in section 3. We have chosen our units such that the background AdS solution is

$$ds^2 = -(1+r^2)dt^2 + \frac{dr^2}{1+r^2} + r^2 d\Omega_3^2, \quad \phi = 0. \quad (2.3)$$

Spherical symmetric solutions will be considered throughout. The general such metric in the ADM decomposition is

$$ds^2 = -N^t(t,r)^2 dt^2 + L(t,r)^2 (dr + N^r(t,r) dt)^2 + R(t,r)^2 d\Omega_3^2. \quad (2.4)$$

It is very convenient to choose $R(t,r) = r$ so that the coordinate r has a clear physical meaning. In our numerical analysis we will be looking for the appearance of trapped surfaces, and we now state the condition for their existence. Consider radial and future directed null geodesics, obeying

$$\frac{dr}{d\lambda} = \left(-N^r \pm \frac{N^t}{L} \right) \frac{dt}{d\lambda}. \quad (2.5)$$

A trapped surface exists whenever $\frac{dr}{d\lambda} < 0$ for either choice of sign. This can be rewritten in a more useful form as follows. Define

$$\mu = r^4 + r^2 - \frac{r^2}{L^2} + \left(\frac{rNr}{Nt}\right)^2. \quad (2.6)$$

μ is proportional to the quasilocal mass, and essentially measures the total amount of energy contained within an S^3 of radius r . If we solve (2.6) for L and substitute into (2.5) we find

$$\frac{dr}{d\lambda} = \left(-Nr \pm \sqrt{(Nr)^2 + \left(1 + r^2 - \frac{\mu}{r^2}\right)(Nt)^2}\right) \frac{dt}{d\lambda}. \quad (2.7)$$

We conclude that trapped surfaces occur for $1 + r^2 - \frac{\mu}{r^2} < 0$. For given constant μ , this is the same as saying that r is inside the horizon of the AdS-Schwarzschild black hole. We will refer to $1 + r^2 - \frac{\mu}{r^2} < 0$ as the ‘‘horizon function’’.

μ was defined above in any coordinate system of the form (2.4) with $R = r$. In our numerical study we will choose to set $N^r = 0$ and write the metric as

$$ds^2 = -n(t, r)^2 \left(1 + r^2 - \frac{\mu(t, r)}{r^2}\right) dt^2 + \frac{dr^2}{1 + r^2 - \frac{\mu(t, r)}{r^2}} + r^2 d\Omega_3^2. \quad (2.8)$$

Setting $n = 1$ and $\mu = \text{constant}$ gives the standard form of the AdS-Schwarzschild black hole, the mass being $M = 3\pi^2\mu$. Since the definition of μ in (2.8) agrees with that in (2.6), we again see that trapped surfaces occur for $1 + r^2 - \frac{\mu}{r^2} < 0$. But given the form of the metric (2.8), it is clear that the coordinates will break down precisely when trapped surfaces are encountered. Therefore in our numerics we will look for $1 + r^2 - \frac{\mu}{r^2}$ becoming very small, and assume that the subsequent evolution is sufficiently smooth that trapped surfaces do indeed occur. We will also give evidence that the trapped surfaces are associated with black hole formation, although it would be interesting to check this directly by using coordinates which can extend into the region containing the trapped surfaces.

With spherical symmetry, the gravitational field has no dynamical degrees of freedom, and the metric functions n and μ on a given time slice can be determined in terms of ϕ and $\dot{\phi}$ evaluated on the same time slice. In particular, two linear combinations of Einstein’s equations yield the constraints

$$\mu' = -\frac{4}{3}r^3\phi^2 + \frac{1}{3}\left(1 + r^2 - \frac{\mu}{r^2}\right)\left(\frac{\pi_\phi^2}{r^3} + r^3(\phi')^2\right), \quad (2.9)$$

$$\frac{n'}{n} = \frac{1}{3r^2}\left(\frac{\pi_\phi^2}{r^3} + r^3(\phi')^2\right). \quad (2.10)$$

Here, π_ϕ is the canonical momentum

$$\pi_\phi = \frac{r^3}{n\left(1 + r^2 - \frac{\mu(t, r)}{r^2}\right)} \dot{\phi}. \quad (2.11)$$

We also need the scalar field equation of motion, which is

$$\begin{aligned} \dot{\pi}_\phi &= \left(r^3\left(1 + r^2 - \frac{\mu}{r^2}\right)n\phi'\right)' + 4r^3n\phi \\ &= n\left(r^3\left(1 + r^2 - \frac{\mu}{r^2}\right)\phi'' + (3r^2 + 5r^4 - \mu + \frac{4}{3}r^4\phi^2)\phi' + 4r^3\phi\right) \end{aligned} \quad (2.12)$$

where (2.9) and (2.10) were used.

For numerical purposes it is useful to redefine variables. We map $r \in [0, \infty]$ to $x \in [-1, 1]$ by

$$r^2 = \frac{1+x}{1-x}. \quad (2.13)$$

The asymptotic behavior of the scalar field can be simplified by defining

$$\psi = (1+r^2)\phi = \frac{2}{1-x}\phi \quad (2.14)$$

$$\pi_\psi = (1-x)^{-1/2}(1+x)^{-3/2}\pi_\phi. \quad (2.15)$$

We now discuss the boundary conditions. In solving (2.9) and (2.10) we can choose the values of μ and n at the origin, and we choose these to be

$$\mu(t, r=0) = \mu(t, x=-1) = 0, \quad n(t, r=0) = n(t, x=-1) = 1. \quad (2.16)$$

Note then that our time coordinate measures the proper time at the origin. As for the scalar field at the origin, we need only demand that ψ is nonsingular there. We also need a boundary condition on the scalar field at infinity. Solving the free scalar field equation in AdS yields the asymptotic behavior

$$\phi \sim \frac{\alpha(t)}{r^2} + \beta(t) \frac{\ln r}{r^2} \quad \Rightarrow \quad \psi(x) \sim \tilde{\alpha}(t) + \tilde{\beta}(t) \ln(1-x). \quad (2.17)$$

The two asymptotic behaviors correspond to the normalizable and non-normalizable modes familiar in the study of fields in AdS. We are allowed to freely specify $\beta(t)$ as well as the values of ϕ and $\dot{\phi}$ on an initial time slice, and then $\alpha(t)$ is determined by the equations of motion (and analogously for ψ , $\tilde{\alpha}$ and $\tilde{\beta}$). Fluctuations around the ordinary AdS vacuum correspond to setting $\beta(t) = \tilde{\beta}(t) = 0$; on the CFT side of the AdS/CFT correspondence this corresponds to evolution with respect to the unperturbed CFT Hamiltonian. We will refer to these boundary conditions as the ‘‘standard’’ ones. Besides the standard boundary conditions, HHM consider a second set of Dirichlet boundary conditions, which we’ll return to in the next section. So, expressed in terms of ψ , the standard boundary conditions just say that ψ should be finite as $x \rightarrow 1$, but is otherwise unrestricted.

The equations of motion can now be written

$$\dot{\psi} = 2 \left(2 - \frac{(1-x)^2}{1+x} \mu \right) n \pi_\psi, \quad (2.18)$$

$$\begin{aligned} \dot{\pi}_\psi &= \frac{1}{2}(1-x) \left(2(1+x) - (1-x)^2 \mu \right) n \psi'' - \left(1 + \frac{(1-x)x}{1+x} \mu \right) n \psi \\ &+ n \left((1-3x) + \frac{(1-x)^2(1+2x)}{1+x} \mu + \frac{1}{6}(1-x)^2(1+x)\psi^2 \right) \psi' \\ &- \frac{1}{6}(1-x)(1+x)n\psi^3, \end{aligned} \quad (2.19)$$

where the metric function n can be expressed as follows

$$n = e^{\int_{-1}^x d\tilde{x} f(\tilde{x})} \quad (2.20)$$

and μ is given by

$$\begin{aligned} \mu = e^{-\int_{-1}^x d\tilde{x} f(\tilde{x})} \int_{-1}^x d\hat{x} \left\{ -\frac{1}{6}(1+\hat{x})\psi^2 + \frac{2}{3}(1+\hat{x})\pi_\psi^2 \right. \\ \left. + \frac{1}{6}(1+\hat{x})^2(1-\hat{x})(\psi')^2 - \frac{1}{3}(1+\hat{x})^2\psi'\psi \right\} e^{\int_{-1}^{\hat{x}} d\tilde{x} f(\tilde{x})} \end{aligned} \quad (2.21)$$

and we defined

$$f = \frac{1}{3} \left((1-x)^2 \pi_\psi^2 + \frac{1}{4} (1-x^2) ((1-x)\psi' - \psi)^2 \right). \quad (2.22)$$

Note that the only potentially singular terms are of the form $\frac{\mu}{1+x}$, but $\mu \sim (1+x)^2$ as $x \rightarrow -1$, so this is not a problem.

Given the way in which μ appears in the metric, its value at infinity gives a natural definition (up to a factor of $3\pi^2$) of the total mass associated with the spacetime. However, for scalar fields which saturate the Breitenlohner-Freedman bound, it turns out that this definition of mass is not conserved. From the definition (2.21) and the equations of motion, one can show

$$\frac{d}{dt} \mu(t, x=1) = -\frac{2}{3} \frac{d}{dt} [\psi(t, x=1)^2]. \quad (2.23)$$

A conserved mass can therefore be defined as

$$m = \mu(t, x=1) + \frac{2}{3} \psi(t, x=1)^2. \quad (2.24)$$

Another important fact is that μ can be negative, while m obeys a positivity theorem.

Following HHM, our initial data will consist of a large homogeneous bubble of scalar field, with vanishing time derivative, and with the standard AdS boundary condition at infinity. So at $t=0$ we have

$$\psi = \frac{2}{1-x} \phi_0 \quad \text{for } x < x_0 \quad (2.25)$$

$$\psi \sim \text{finite} \quad \text{for } x \rightarrow 1 \quad (2.26)$$

$$\pi_\psi = 0 \quad (2.27)$$

with ϕ_0 being the constant value of ϕ inside the bubble. We take the bubble to be sufficiently large that a singularity is guaranteed to form at the center of the bubble within finite time.¹ Furthermore, we restrict the size of the bubble and the scalar field profile outside the bubble to be such that the asymptotic value of μ is negative. Were μ conserved this initial data would certainly evolve to a naked singularity, since black holes have $\mu > 0$. However, we know that μ is not conserved, and the question becomes whether it can increase sufficiently rapidly to allow a black hole to form before a naked singularity appears; we will see that this is indeed what happens.

3. Results

We solve the equations (2.18) and (2.19) numerically using C code by evaluating the integrals for n and μ on a given time slice, and then evolving ψ and π_ψ forward by a simple

¹See [15] for a discussion of the required size.

time stepping. We take the number of spatial lattice points to be a few thousand. Stability requires that the time step is approximately the square of the spatial lattice spacing, and we have taken $dt = dx^2/2$. We have done the numerical evolution using various number of lattice points, and a refinement of the lattice does not show any sign of a numerical instability. In the course of the evolution $n(x, t)$ becomes very large near the boundary. In order to avoid a numerical instability we have to adjust the time stepping $dt \rightarrow dt/n(t, x)$. We evolve in time until the numerics break down, which occurs when the horizon function $1 + r^2 - \frac{\mu}{r^2}$ becomes very small, and this is associated with the appearance of trapped surfaces.

3.1 Standard boundary conditions

With 4001 lattice points, we have chosen various values for ϕ_0 and x_0 in the initial data. Outside the bubble, the initial data for ψ is taken to be linear in x , with slope matched to the first derivative of ψ just inside the bubble. In the following we will present the results for two cases. In the first we present a fairly generic example using the potential 2.2, and in the second we instead use the full supergravity potential.

Case 1. Quadratic potential: For $x_0 = .583$ and $\phi_0 = 0.2$, we find that our numerics break down at $t_{final} = 0.8837$. The initial profile of $\psi(x)$ is given by Fig. 1

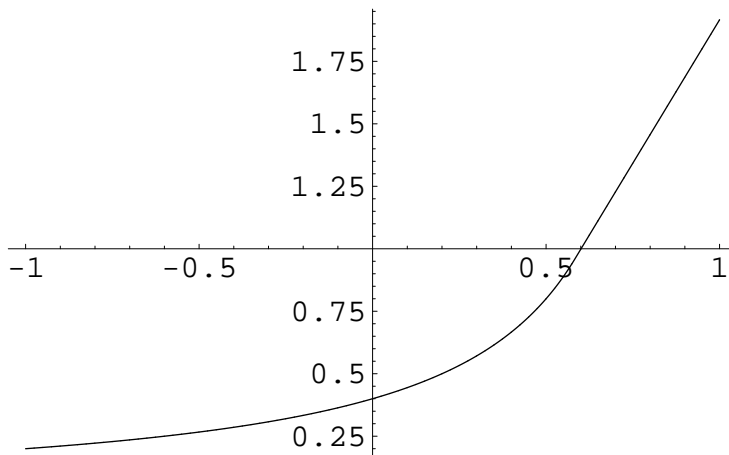


Figure 1: Initial profile of $\psi(x)$ at $t = 0$

whereas the final profile is given by Fig. 2

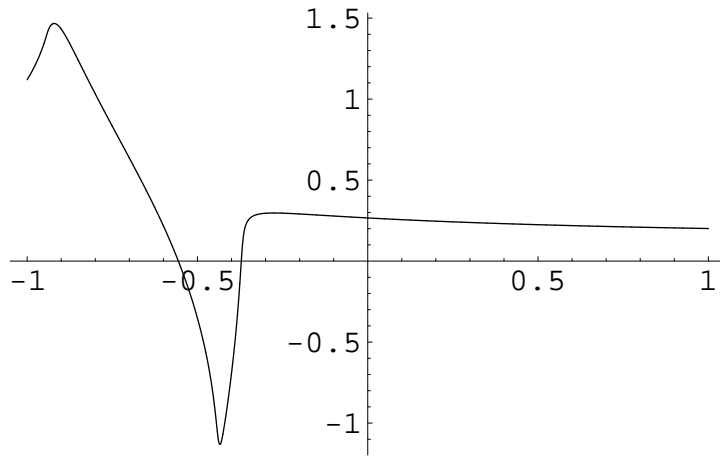


Figure 2: Final profile of $\psi(x)$ at $t = t_{final}$

The plot of the conserved mass $m(t)$ versus nonconserved mass $\mu(t)$ in Fig. 3 reveals that indeed $m(t)$ is conserved all the way to t_{final} . The fact that $m(t)$ is conserved to great accuracy all the way to $t = t_{final}$ constitutes a good check of our numerics.

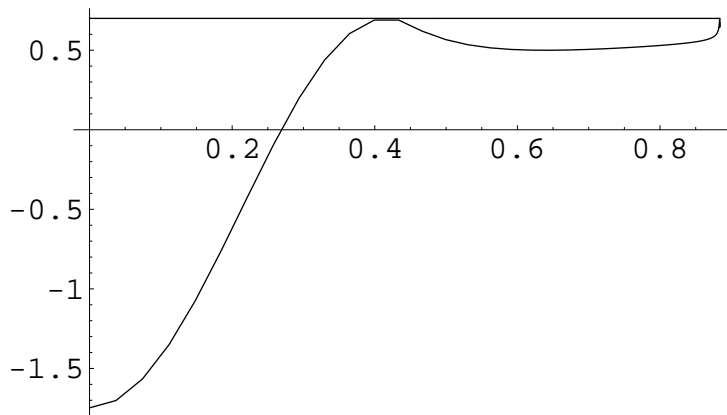


Figure 3: Conserved mass versus nonconserved mass as functions of time

As discussed in section 2, the vanishing of the horizon function $1 + r^2 - \mu/r^2$ indicates the occurrence of a horizon (or more accurately an apparent horizon) at $x_h = -0.376$, as seen in Fig. 4

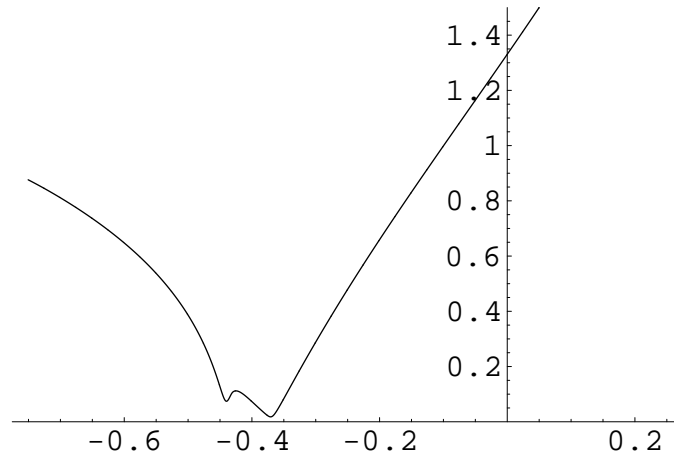


Figure 4: Horizon function at $t = t_{final}$

The Ricciscalar remains well behaved near $x = x_h$, although it grows in the region $x < x_h$. At $t = t_{final}$ the Ricciscalar is shown in Fig. 5

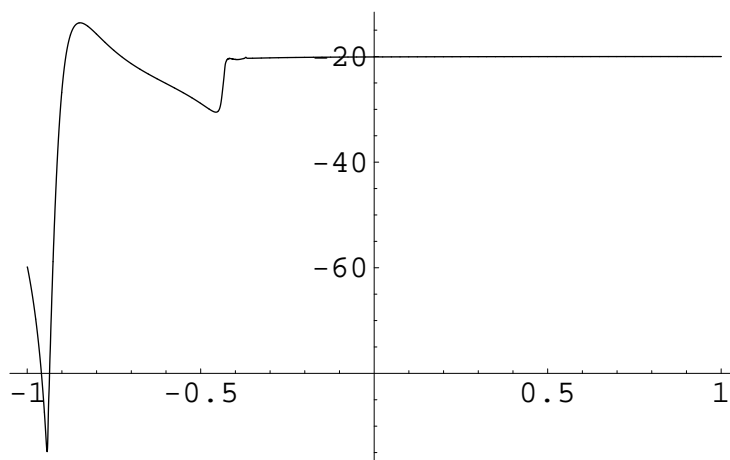


Figure 5: Ricciscalar at $t = t_{final}$

Case 2. Supergravity potential: The quadratic potential (2.2) for the scalar field ϕ is an approximation to the exact supergravity potential

$$V(\phi) = -2 \exp\left(\frac{2}{\sqrt{3}}\phi\right) - 4 \exp\left(-\frac{1}{\sqrt{3}}\phi\right) + 6 \quad (3.1)$$

Numerically, this is more expensive to evaluate. For the same initial data as shown in Fig.1, with $x_0 = 0.583$ and $\phi_0 = 0.2$ and 2001 lattice points, the numerical evolution breaks down after $t_{final} = 0.8217$. The results are very similar to the ones for the quadratic potential. The final profile is plotted in Fig. 6.

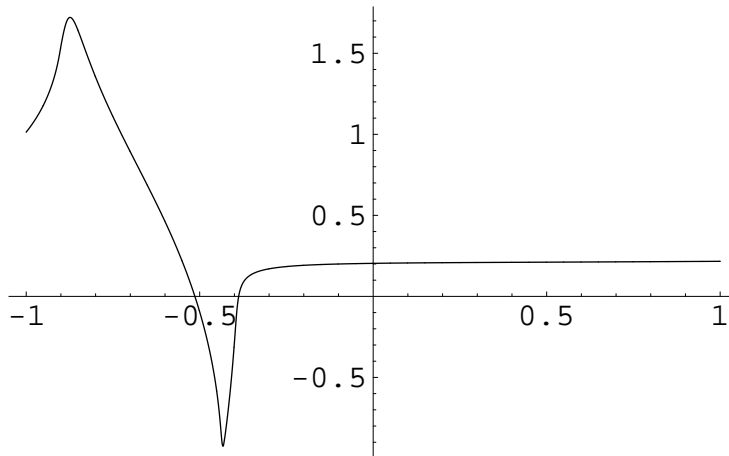


Figure 6: Final profile of $\psi(x)$ at $t = t_{final}$

The horizon function at $t = T_{final}$, as plotted in Fig. 7, indicates that the horizon forms near $x_h = -0.41$.

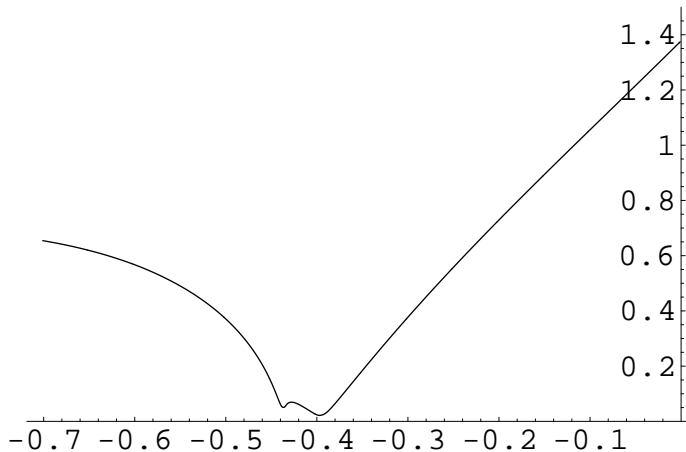


Figure 7: Horizon function at $t = t_{final}$

Hence the full nonlinear potential displays the same characteristic features as the quadratic potential.

These two numerical results are a sample of the generic features of almost all initial configurations we have studied. The nonconserved mass rapidly becomes positive and an apparent horizon forms. The size of the horizon grows with the conserved mass, and we have studied initial data where the horizon radius is considerably larger than 1. We interpret the apparent horizon to be associated with black hole formation since it appears well outside the bubble in a region where the curvature seems to remain small. In particular, we are distinguishing our trapped surface from those trapped surfaces which we know will appear in the homogeneous region of the bubble as the singularity is approached; the latter have nothing directly to do with black hole formation.

We also seem to find the first indications for the decay of the scalar field, in line with the no-hair theorem, and a likely endpoint of the evolution is an AdS-Schwarzschild black hole without scalar hair. However, since our numerics break down when the horizon forms, one has to use more sophisticated numerical methods to settle this question. In any case, it seems clear that cosmic censorship is not violated in this setup.

3.2 Dirichlet boundary conditions

HHM have proposed a second scenario for producing naked singularities, which involves imposing Dirichlet boundary conditions at some large but finite radius, $r = R_1$.² We take constant $\phi = \phi_0$ inside a bubble of radius R_0 , and set $\phi(R_1) = \phi_1$. To minimize the energy we take $\phi(r)$ to obey the linearized equations of motion outside the bubble:

$$\begin{aligned} \phi &= \phi_0 & (r < R_0) \\ \phi &= \frac{a}{r^2} + b \frac{\ln(1+r^2)}{r^2} & (R_0 < r < R_1) \end{aligned} \quad (3.2)$$

where a and b are determined by the boundary conditions at R_0 and R_1 . HHM actually consider slightly different initial data which do not satisfy the equations of motion outside the bubble, but we consider 3.2 since it will clearly give lower mass and thus be more favorable for violating cosmic censorship.

We will reduce to a three parameter family of initial data by minimizing the mass with respect to ϕ_0 while holding R_0, R_1 and ϕ_1 fixed. This yields the mass formula

$$\mu_{\text{initial}} = -\frac{2}{3}\phi_1^2 R_1^2 \left(1 + R_1^2 \left(1 - \frac{2 + R_0^2}{(2 + R_0^2) \ln(1 + R_1^2) - (2 + R_0^2) \ln(1 + R_0^2) + 2R_0^2} \right) \right). \quad (3.3)$$

Following HHM, we further require $\phi_0 \ll 1$ so as to be able to neglect backreaction. In this regime, HHM show that if a black hole forms then the size of the event horizon on the initial surface must be at least $\phi_0^{2/3} R_0$.

For $R_1 \gg R_0 \gg 1$, which HHM consider, we have $\mu_{\text{initial}} < 0$, and μ is conserved due to the Dirichlet boundary condition. But to establish a violation of cosmic censorship one needs to further argue that any black hole obeying the same Dirichlet condition at R_1 , and with horizon size at least $\phi_0^{2/3} R_0$, has $\mu_{\text{bh}} > \mu_{\text{initial}}$.

²We thank Thomas Hertog and Gary Horowitz for discussions regarding the material in this section.

We therefore look for static black hole solutions, satisfying

$$\begin{aligned} \mu' + \frac{4}{3}r^2\phi^2 - \frac{1}{3}\left(1 + r^2 - \frac{\mu}{r^2}\right)r^3(\phi')^2 &= 0 \\ r^2\left(1 + r^2 - \frac{\mu}{r^2}\right)\phi'' + (3r^2 + 5r^4 - \mu + \frac{4}{3}r^4\phi^2)\phi' + 4r^3\phi &= 0. \end{aligned} \quad (3.4)$$

We take the horizon to be at $r = R_s$, and so $\mu(R_s) = R_s^4 + R_s^2$. The equations of motion can be seen to fix $\phi'(R_s)$ in terms of $\phi(R_s)$, and so the black hole solution is completely specified by R_s , R_1 and ϕ_1 . We numerically integrate the equations outward from the horizon to R_1 , and then adjust R_s and $\phi(R_s)$ so as to satisfy $\phi(R_1) = \phi_1$. We also have to satisfy $R_s > \phi_0^{2/3}R_0$ in order to be sure that our horizon is large enough to enclose the region in which we know singularities will form. Although we were able to use the free field approximation to compute the mass of the bubble, it turns out that backreaction is quantitatively important for the black hole, and so we are forced to solve the full nonlinear equations 3.4.

We have carried out this procedure for a few parameter choices, as summarized below.

Example 1: We take

$$R_1 = 20000, \quad R_0 = 100, \quad \phi_1 = 10^{-6}. \quad (3.5)$$

Then $\phi_0 = 0.006$, hence the backreaction for the bubble can indeed be neglected. The mass of the bubble is then $\mu_{\text{initial}} = -98198.5$ and the critical horizon radius is $\phi_0^{2/3}R_0 = 3.429$. We then succeed in finding a black hole solution with $R_s = 4$ and $\mu_{\text{bh}} = -100165$. Since $\mu_{\text{bh}} < \mu_{\text{initial}}$ the energetics allow black hole formation, and so there is no reason to expect cosmic censorship to be violated.

Example 2: We take

$$R_1 = 100000, \quad R_0 = 500, \quad \phi_1 = 10^{-7} \quad (3.6)$$

yielding $\mu_{\text{initial}} = -613742$, and the critical horizon radius is $\phi_0^{2/3}R_0 = 3.699$. We then find a black hole solution with $R_s = 6$ and $\mu_{\text{bh}} = -630601$. So we again find $\mu_{\text{bh}} < \mu_{\text{initial}}$.

It is possible that there exists some other choice of parameters such that $\mu_{\text{bh}} > \mu_{\text{initial}}$, but we have not encountered such a case so far.

Now we turn to the numerical time evolution in the Dirichlet case. Using our variables, the regime $\ln R_1 / \ln R_0 \gg 1$ considered by HHM is rather inaccessible due to the large hierarchy of scales. We will instead consider similar initial data as we studied in the case of standard boundary conditions, and return to the $\ln R_1 / \ln R_0 \gg 1$ case in a future publication.

For the numerical evolution we chose initial data with $x_0 = 0.583$, $\phi_0 = 0.2$, and with 3981 lattice points. The Dirichlet boundary condition is imposed at $x_1 = 0.99$. The numerical evolution breaks down at $t_{\text{final}} = 0.9139$.

The initial profile of $\psi(x)$ is shown in Fig. 8

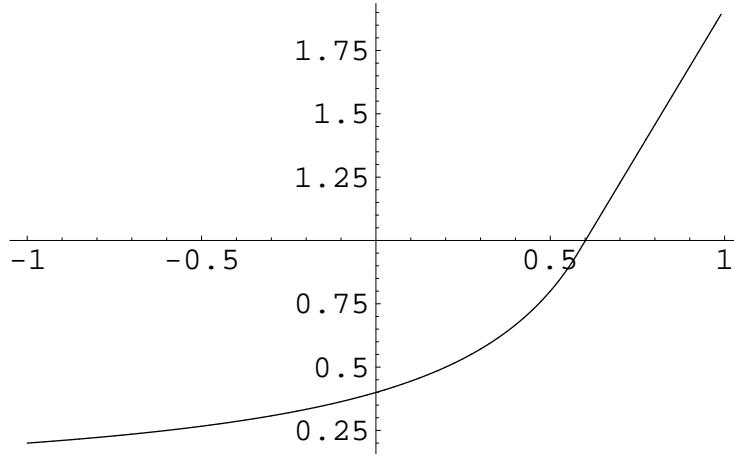


Figure 8: Initial profile of $\psi(x)$ at $t = 0$

and the final profile is shown in Fig. 9.

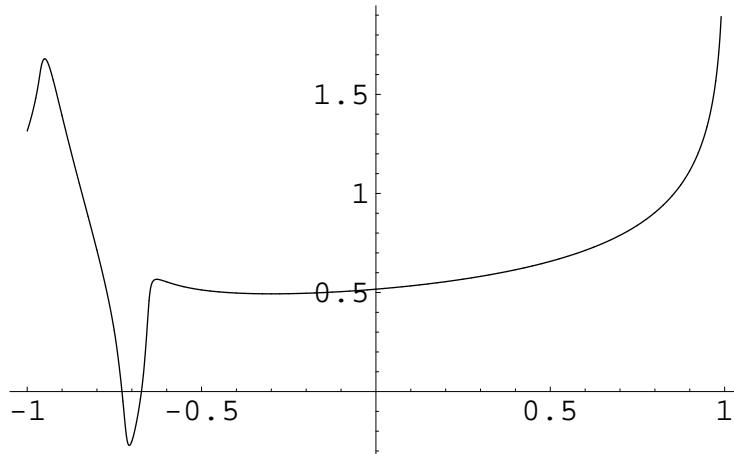


Figure 9: Final profile of $\psi(x)$ at $t = t_{final}$

The horizon function at $t = t_{final}$ is plotted in Fig. 10, and the Ricciscalar is well be-

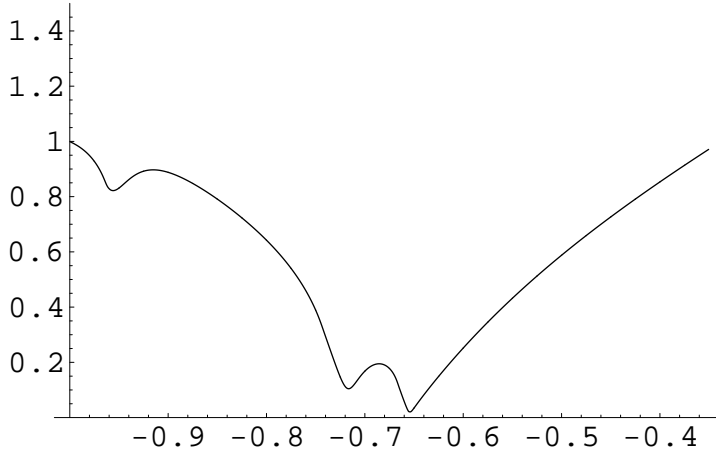


Figure 10: Horizon function at $t = t_{final}$

haved near the horizon. We have also checked that the mass is conserved to excellent accuracy. The approximate vanishing of the horizon function indicates that the evolution with Dirichlet boundary conditions leads to a singularity shielded by a horizon instead of a naked singularity.

4. Discussion

We have given evidence that cosmic censorship survives the challenge from collapsing bubbles of Breitenlohner-Freedman mass scalar fields in AdS. In particular, the existence of negative mass for the initial data is consistent with black hole formation since the mass becomes positive rather early in the evolution. In the case of Dirichlet boundary conditions there is still a possibility of violating cosmic censorship since we have not exhausted the full parameter space. However, we should point out that if one truly wishes to form a naked singularity in *string theory* then we are presumably restricted to the standard boundary conditions; being a quantum theory of gravity, string theory only admits asymptotic boundary conditions and not Dirichlet conditions at finite locations.

There have been a number of previous numerical studies of the dynamics of scalar fields coupled to gravity in AdS spacetimes [19][20]. In these papers the main focus was on massless scalar fields. The study of gravitational collapse and black hole/singularity formation using numerical techniques is a very interesting problem in general.

In the future we hope to study various different scalar field potentials, for example those considered in [16][21], and to employ coordinates which continue through the horizon of the black hole. Our numerics were based on the simplest discretization and evolution schemes, and it would be interesting to apply more sophisticated techniques like mesh refinement or excision to this problem and check our results. In particular it would be interesting to investigate the critical phenomena associated with gravitational collapse (see [22][23] for reviews) in the context of the AdS/CFT correspondence.

Acknowledgments

We thank Thomas Hertog, Gary Horowitz, Veronika Hubeny, Juan Maldacena, and Steve Shenker for discussions. The work of MG is supported in part by NSF grant 0245096, and the work of PK is supported in part by NSF grant 0099590. Any opinions, findings and conclusions expressed in this material are those of the authors and do not necessarily reflect the views of the National Science Foundation.

References

- [1] R. Penrose, “Gravitational Collapse: The Role Of General Relativity,” *Riv. Nuovo Cim.* **1**, 252 (1969) [*Gen. Rel. Grav.* **34**, 1141 (2002)].
- [2] V. Balasubramanian, S. F. Hassan, E. Keski-Vakkuri and A. Naqvi, “A space-time orbifold: A toy model for a cosmological singularity,” *Phys. Rev. D* **67** (2003) 026003 [arXiv:hep-th/0202187].
- [3] H. Liu, G. Moore and N. Seiberg, “Strings in a time-dependent orbifold,” *JHEP* **0206**, 045 (2002) [arXiv:hep-th/0204168].
- [4] H. Liu, G. Moore and N. Seiberg, “Strings in time-dependent orbifolds,” *JHEP* **0210**, 031 (2002) [arXiv:hep-th/0206182].
- [5] B. Craps, D. Kutasov and G. Rajesh, “String propagation in the presence of cosmological singularities,” *JHEP* **0206** (2002) 053 [arXiv:hep-th/0205101].
- [6] M. Fabinger and J. McGreevy, “On smooth time-dependent orbifolds and null singularities,” *JHEP* **0306** (2003) 042 [arXiv:hep-th/0206196].
- [7] L. Cornalba and M. S. Costa, “A new cosmological scenario in string theory,” *Phys. Rev. D* **66**, 066001 (2002) [arXiv:hep-th/0203031].
- [8] L. Cornalba, M. S. Costa and C. Kounnas, “A resolution of the cosmological singularity with orientifolds,” *Nucl. Phys. B* **637**, 378 (2002) [arXiv:hep-th/0204261].
- [9] M. Gutperle and A. Strominger, “Spacelike branes,” *JHEP* **0204**, 018 (2002) [arXiv:hep-th/0202210].
- [10] J. M. Maldacena, “Eternal black holes in Anti-de-Sitter,” *JHEP* **0304** (2003) 021 [arXiv:hep-th/0106112].
- [11] P. Kraus, H. Ooguri and S. Shenker, “Inside the horizon with AdS/CFT,” *Phys. Rev. D* **67**, 124022 (2003) [arXiv:hep-th/0212277].
- [12] L. Fidkowski, V. Hubeny, M. Kleban and S. Shenker, “The black hole singularity in AdS/CFT,” arXiv:hep-th/0306170.
- [13] G. T. Horowitz and J. Maldacena, “The black hole final state,” arXiv:hep-th/0310281.
- [14] D. Gottesman and J. Preskill, “Comment on ‘The black hole final state’,” arXiv:hep-th/0311269.
- [15] T. Hertog, G. T. Horowitz and K. Maeda, “Negative energy in string theory and cosmic censorship violation,” arXiv:hep-th/0310054.
- [16] T. Hertog, G. T. Horowitz and K. Maeda, “Generic cosmic censorship violation in anti de Sitter space,” arXiv:gr-qc/0307102.

- [17] P. Breitenlohner and D. Z. Freedman, “Stability In Gauged Extended Supergravity,” *Annals Phys.* **144**, 249 (1982).
- [18] P. Breitenlohner and D. Z. Freedman, “Positive Energy In Anti-De Sitter Backgrounds And Gauged Extended Supergravity,” *Phys. Lett. B* **115**, 197 (1982).
- [19] F. Pretorius and M. W. Choptuik, “Gravitational collapse in 2+1 dimensional AdS spacetime,” *Phys. Rev. D* **62**, 124012 (2000) [arXiv:gr-qc/0007008].
- [20] V. Husain, G. Kunstatter, B. Preston and M. Birukou, “Anti-deSitter gravitational collapse,” *Class. Quant. Grav.* **20**, L23 (2003) [arXiv:gr-qc/0210011].
- [21] M. Alcubierre, J. A. Gonzalez, M. Salgado and D. Sudarsky, “The cosmic censor conjecture: Is it generically violated?,” arXiv:gr-qc/0402045.
- [22] C. Gundlach, “Critical phenomena in gravitational collapse,” *Phys. Rept.* **376** (2003) 339 [arXiv:gr-qc/0210101].
- [23] M. W. Choptuik, “Critical Behaviour In Gravitational Collapse,” *Prog. Theor. Phys. Suppl.* **136** (1999) 353.